

SUPPLEMENTARY METHODS*Library preparation*

Library preparation was carried out using either poly-A enrichment or ribosomal RNA depletion. For *Tidestromia oblongifolia*, tissue collection, RNA isolation, library preparation was carried out using the KAPA Stranded mRNA-Seq Kits (KAPA Biosystems, Wilmington, Massachusetts, USA). The library was multiplexed with 10 other samples from a different project on an Illumina HiSeq2500 platform with V4 chemistry at the University of Michigan Sequencing Core. For the remaining 16 samples total RNA was isolated from c. 70-125 mg leaf tissue collected in liquid nitrogen using the RNeasy Plant Mini Kit (Qiagen) following the manufacturer's protocol (June 2012). A DNase digestion step was included with the RNase-Free DNase Set (Qiagen). Quality and quantity of RNA were checked using the 2100 Bioanalyzer (Agilent Technologies). Library preparation was carried out using the TruSeq® Stranded Total RNA Library Prep Plant with RiboZero probes (96 Samples, Illumina, #20020611; Schuierer et al. 2017). Indexed libraries were normalized, pooled and size selected to 320bp +/- 5% using the Pippin Prep HT instrument to generate libraries with mean inserts of 200 bp, and sequenced on the Illumina HiSeq2500 platform with V4 chemistry at the University of Minnesota Genomics Center. Reads from all 17 libraries were paired-end 125 bp.

Transcriptome data processing and assembly

Scripts and instructions for read processing, assembly, translation, and homology and orthology search can be found at https://bitbucket.org/yanglab/phylogenomic_dataset_construction/ as part of an updated ‘phylogenomic dataset construction’ pipeline (Yang and Smith 2014).

We processed raw reads for all 88 transcriptome datasets (except *Bienertia sinuspersici*) used in this study (Table S1). Sequencing errors in raw reads were corrected with Rcorrector (Song and Florea 2015) and reads flagged as uncorrectable were removed. Sequencing adapters and low-quality bases were removed with Trimmomatic v0.36 (ILLUMINACLIP: TruSeq_ADAPTER: 2:30:10 SLIDINGWINDOW: 4:5 LEADING: 5 TRAILING: 5 MINLEN: 25; Bolger et al. 2014). Additionally, chloroplast and mitochondrial reads were filtered with Bowtie2 v 2.3.2 (Langmead and Salzberg 2012) using publicly available Caryophyllales organelle genomes from the Organelle Genome Resources database (RefSeq; [Pruitt et al. 2007]; last accessed on October 17, 2018) as references. Read quality was assessed with FastQC v 0.11.7 (<https://www.bioinformatics.babraham.ac.uk/projects/fastqc/>). Overrepresented sequences detected with FastQC were discarded. *De novo* assembly was carried out with Trinity v 2.5.1 (Grabherr et al. 2011) with default settings, but without in silico normalization. Assembly quality was assessed with Transrate v 1.0.3 (Smith-Unna et al. 2016). Low quality and poorly supported transcripts were removed using individual cut-off values for three contig score components of Transrate: 1) proportion of nucleotides in a contig that agrees in identity with the aligned read, $s(\text{Cnuc}) \leq 0.25$; 2) proportion of nucleotides in a contig that have one or more mapped reads, $s(\text{Ccov}) \leq 0.25$; and 3) proportion of reads that map to the contig in correct orientation, $s(\text{Cord}) \leq 0.5$. Furthermore, chimeric transcripts (*trans-self* and *trans-multi-gene*) were removed following the approach described in Yang and Smith (2013) using *Beta vulgaris* as the reference proteome,

and percentage similarity and length cutoffs of 30 and 100, respectively. In order to remove isoforms and assembly artifacts, filtered reads were remapped to filtered transcripts with Salmon v 0.9.1 (Patro et al. 2017) and putative genes were clustered with Corset v 1.07 (Davidson and Oshlack 2014) using default settings, except that we used a minimum of five reads as threshold to remove transcripts with low coverage (-m 5). Only the longest transcript of each putative gene inferred by Corset was retained (Chen et al. 2019). Filtered transcripts were translated with TransDecoder v 5.0.2 (Haas et al. 2013) with default settings and the proteome of *Beta vulgaris* and *Arabidopsis thaliana* to identify open reading frames. Finally, coding sequences (CDS) from translated amino acids were further reduced with CD-HIT v 4.7 (-c 0.99; [Fu et al. 2012]) to remove near-identical sequences.

Homology and orthology inference of nuclear genes

Initial homology inference was carried out following Yang and Smith (2014) with some modifications. First, an all-by-all BLASTN search was performed on CDS using an *E* value cutoff of 10 and max_target_seqs set to 100. Raw BLAST output was filtered with a hit fraction of 0.4. Then putative homologs groups were clustered using MCL v 14-137 (van Dongen 2000) with a minimum minus log-transformed *E* value cutoff of 5 and an inflation value of 1.4. Finally, only clusters with a minimum of 25 taxa were retained. Individual clusters were aligned using MAFFT v 7.307 (Katoh and Standley 2013) with settings ‘-genafpair -maxiterate 1000’. Aligned columns with more than 90% missing data were removed using Phyx (Brown et al. 2017). Homolog trees were built using RAxML v 8.2.11 (Stamatakis 2014) with a GTRCAT model and clade support assessed with 200 rapid bootstrap (BS) replicates. Spurious or outlier long tips were detected and removed with TreeShrink v 1.0.0. by maximally reducing the tree

diameter (Mai and Mirarab 2018). Monophyletic and paraphyletic tips that belonged to the same taxon were removed keeping the tip with the highest number of characters in the trimmed alignment. After visual inspection of ca. 50 homolog trees, we determined that internal branches longer than 0.25 were likely representing deep paralogs. These branches were cut apart, keeping resulting subclades with a minimum of 25 taxa. Homolog tree inference, tip and outlier removal, and deep paralog cutting was carried out for a second time using the same settings to obtain final homologs. Orthology inference was carried out following the ‘monophyletic outgroup’ approach from Yang and Smith (2014), keeping only ortholog groups with at least 25 ingroup taxa. The ‘monophyletic outgroup’ approach filters for clusters that have outgroup taxa being monophyletic and single-copy, and therefore filters for single- and low-copy genes. It then roots the gene tree by the outgroups, traverses the rooted tree from root to tip, and removes the side with less taxa when gene duplication is detected.

Synteny analyses

To visualize any genomic patterns of the phylogenetic history of *Beta vulgaris* regarding its relationship with Amaranthaceae s.s. and Chenopodiaceae, we first identified syntenic regions between the genomes of *Beta vulgaris* and the outgroup *Mesembryanthemum crystallinum* using the SynNet pipeline (<https://github.com/zhaotao1987/SynNet-Pipeline>; Zhao and Schranz 2019). We used DIAMOND v.0.9.24.125 (Buchfink et al. 2015) to perform all-by-all inter- and intra-pairwise protein searches with default parameters, and MCSanX (Wang et al. 2012) for pairwise syntenic block detection with default parameters, except match score (-k) that was set to five. Then, we plot the nine chromosomes of *Beta vulgaris* by assigning each of the 8,258 orthologs of the quartet composed of *Mesembryanthemum crystallinum* (outgroup), *Amaranthus*

hypochondriacus, *Beta vulgaris*, and *Chenopodium quinoa* (BC1A) to synteny blocks and to one of the three possible quartet topologies based on best likelihood score.

Assessment of substitutional saturation, codon usage bias, compositional heterogeneity, and model of sequence evolution misspecification

We refiltered the final 105-taxon ortholog alignments to again include genes that have the same 11 taxa (referred herein as 11-taxon(tree) dataset used for the species network analyses. We realigned individual genes using MACSE v.2.03 (Ranwez et al. 2018) to account for codon structure and frameshifts. Codons with frameshifts were replaced with gaps, and ambiguous alignment sites were removed using GBLOCKS v0.9b (Castresana 2000) while accounting for codon alignment (-t=c -b1=6 -b2=6 -b3=2 -b4=2 -b5=h). After realignment and removal of ambiguous sites, we kept genes with a minimum of 300 aligned base pairs. To detect potential saturation, we plotted the uncorrected genetic distances against the inferred distances as described in Philippe and Forterre (1999). The level of saturation was determined by the slope of the linear regression between the two distances where a shallow slope (i.e < 1) indicates saturation. We estimated the level of saturation by concatenating all genes and dividing the first and second codon positions from the third codon positions. We calculated uncorrected, and inferred distances with the TN93 substitution model using APE v5.3 (Paradis and Schliep 2019) in R. To determine the effect of saturation in the phylogenetic inferences we estimated individual gene trees using three partition schemes. We inferred ML trees with an unpartitioned alignment, a partition by first and second codon positions, and the third codon positions, and by removing all third codon positions. All tree searches were carried out in RAxML with a GTRGAMMA model and 200 bootstrap replicates. A species tree for each of the three data schemes was

estimated with ASTRAL-III v5.6.3 (Zhang et al. 2018) and gene tree discordance was examined with PhyParts (Smith et al. 2015).

Codon usage bias was evaluated using a correspondence analysis of the Relative Synonymous Codon Usage (RSCU), which is defined as the number of times a particular codon is observed relative to the number of times that the codon would be observed in the absence of any codon usage bias (Sharp and Li 1986). RSCU for each codon in the 11-taxon concatenated alignment was estimated with CodonW v.1.4.4 (Peden 1999). Correspondence analysis was carried out using FactoMineR v1.4.1(Lê et al. 2008) in R (R Core Team 2019). . To determine the effect of codon usage bias in the phylogenetic inferences we estimated individual gene trees using codon-degenerated alignments. Alignments were recoded to eliminate signals associated with synonymous substitutions by degenerating the first and third codon positions using ambiguity coding using DEGEN v1.4 (Regier et al. 2010; Zwick et al. 2012). Gene tree inference and discordance analyses were carried out on the same three data schemes as previously described.

To examine the presence of among-lineage compositional heterogeneity, individual genes were evaluated using the compositional homogeneity test that uses a null distribution from simulations as proposed by Foster (2004). We performed the compositional homogeneity test by optimizing individual gene trees with a GTRGAMMA model and 1,000 simulations in P4 (Foster 2004). To assess if compositional heterogeneity had an effect in species tree inference and gene tree discordance, gene trees that showed the signal of compositional heterogeneity were removed from saturation and codon usage analyses and the species tree and discordance analyses were rerun.

To explore the effect of sequence evolution model misspecification, we reanalyzed the datasets from the saturation and codon usage analyses using inferred gene trees that accounted for model selection. We performed extended model selection followed by ML gene tree inference and 1,000 ultrafast bootstrap replicates for branch support in IQ-Tree v.1.6.1 (Nguyen et al. 2015). Species tree inference, conflict analysis and removal of genes with compositional heterogeneity were carried out as previously described.

Finally, we also used amino acid alignments from MACSE to account for substitutional saturation. Amino acid positions with frameshifts were replaced with gaps, and ambiguous alignment sites were removed with Phyx requiring a minimal occupancy of 30%. We inferred individual gene trees with IQ-tree to account for a model of sequence evolution and carried out species tree inference, conflict analysis, and removal of genes with compositional heterogeneity as described for the nucleotide alignments.

REFERENCES

- Bolger A.M., Lohse M., Usadel B. 2014. Trimmomatic - a flexible trimmer for Illumina sequence data. *Bioinformatics*. 30:2112–2120.
- Brown J.W., Walker J.F., Smith S.A. 2017. Phyx - phylogenetic tools for unix. *Bioinformatics*. 33:1886–1888.
- Buchfink B., Xie C., Huson D.H. 2015. Fast and sensitive protein alignment using DIAMOND. *Nat. Methods*. 12:59–60.
- Castresana J. 2000. Selection of Conserved Blocks from Multiple Alignments for Their Use in Phylogenetic Analysis. *Mol. Biol. Evol.* 17:540–552.

- Chen L.-Y., Morales-Briones D.F., Passow C.N., Yang Y. 2019. Performance of gene expression analyses using de novo assembled transcripts in polyploid species. *Bioinformatics*. 35:4314–4320
- van Dongen S.M. 2000. Graph Clustering by Flow Simulation. PhD diss., Utrecht University.
- Davidson N.M., Oshlack A. 2014. Corset: enabling differential gene expression analysis for de novo assembled transcriptomes. *Genome Biol.* 15:57.
- Foster P.G. 2004. Modeling Compositional Heterogeneity. *Syst. Biol.* 53:485–495.
- Fu L., Niu B., Zhu Z., Wu S., Li W. 2012. CD-HIT: accelerated for clustering the next-generation sequencing data. *Bioinformatics*. 28:3150–3152.
- Grabherr M.G., Haas B.J., Yassour M., Levin J.Z., Thompson D.A., Amit I., Adiconis X., Fan L., Raychowdhury R., Zeng Q., Chen Z., Mauceli E., Hacohen N., Gnirke A., Rhind N., di Palma F., Birren B.W., Nusbaum C., Lindblad-Toh K., Friedman N., Regev A. 2011. Full-length transcriptome assembly from RNA-Seq data without a reference genome. *Nat. Biotechnol.* 29:644–652.
- Haas B.J., Papanicolaou A., Yassour M., Grabherr M., Blood P.D., Bowden J., Couger M.B., Eccles D., Li B., Lieber M., MacManes M.D., Ott M., Orvis J., Pochet N., Strozzi F., Weeks N., Westerman R., William T., Dewey C.N., Henschel R., LeDuc R.D., Friedman N., Regev A. 2013. *De novo* transcript sequence reconstruction from RNA-seq using the Trinity platform for reference generation and analysis. *Nat. Protoc.* 8:1494–1512.
- Katoh K., Standley D.M. 2013. MAFFT Multiple Sequence Alignment Software Version 7: Improvements in Performance and Usability. *Mol. Biol. Evol.* 30:772–780.
- Langmead B., Salzberg S.L. 2012. Fast gapped-read alignment with Bowtie 2. *Nat. Methods*. 9:357–359.

- Lê S., Josse J., Husson F. 2008. FactoMineR : An R Package for Multivariate Analysis. *J. Stat. Softw.* 25: 1–18.
- Mai U., Mirarab S. 2018. TreeShrink: fast and accurate detection of outlier long branches in collections of phylogenetic trees. *BMC Genomics.* 19:4046.
- Nguyen L.-T., Schmidt H.A., von Haeseler A., Minh B.Q. 2015. IQ-TREE: A Fast and Effective Stochastic Algorithm for Estimating Maximum-Likelihood Phylogenies. *Mol. Biol. Evol.* 32:268–274.
- Paradis E., Schliep K. 2019. ape 5.0: an environment for modern phylogenetics and evolutionary analyses in R. *Bioinformatics.* 35:526–528.
- Patro R., Duggal G., Love M.I., Irizarry R.A., Kingsford C. 2017. Salmon provides fast and bias-aware quantification of transcript expression. *Nat. Methods.* 14:417–419.
- Peden J. 1999. Analysis of Codon Usage. PhD diss., University of Nottingham.
- Pruitt K.D., Tatusova T., Maglott D.R. 2007. NCBI reference sequences (RefSeq): a curated non-redundant sequence database of genomes, transcripts and proteins. *Nucleic Acids Res.* 35:D61–D65.
- Philippe H., Forterre P. 1999. The Rooting of the Universal Tree of Life Is Not Reliable. *J. Mol. Evol.* 49:509–523.
- R Core Team. 2019. R: A Language and Environment for Statistical Computing. Vienna, Austria: R Foundation for Statistical Computing.
- Ranwez V., Douzery E.J.P., Cambon C., Chantret N., Delsuc F. 2018. MACSE v2: Toolkit for the Alignment of Coding Sequences Accounting for Frameshifts and Stop Codons. *Mol. Biol. Evol.* 35:2582–2584.

- Regier J.C., Shultz J.W., Zwick A., Hussey A., Ball B., Wetzler R., Martin J.W., Cunningham C.W. 2010. Arthropod relationships revealed by phylogenomic analysis of nuclear protein-coding sequences. *Nature*. 463:1079–1083.
- Schuijjer S., Carbone W., Knehr J., Petitjean V., Fernandez A., Sultan M., Roma G. 2017. A comprehensive assessment of RNA-seq protocols for degraded and low-quantity samples. *BMC Genomics*. 18:442.
- Smith S.A., Moore M.J., Brown J.W., Yang Y. 2015. Analysis of phylogenomic datasets reveals conflict, concordance, and gene duplications with examples from animals and plants. *BMC Evol. Biol.* 15:745.
- Smith-Unna R., Boursnell C., Patro R., Hibberd J.M., Kelly S. 2016. TransRate: reference-free quality assessment of de novo transcriptome assemblies. *Genome Res*. 26:1134–1144.
- Song L., Florea L. 2015. Rcorrector: efficient and accurate error correction for Illumina RNA-seq reads. *GigaScience*. 4:48.
- Stamatakis A. 2014. RAxML version 8 - a tool for phylogenetic analysis and post-analysis of large phylogenies. *Bioinformatics*. 30:1312–1313.
- Wang Y., Tang H., DeBarry J.D., Tan X., Li J., Wang X., Lee T. -h., Jin H., Marler B., Guo H., Kissinger J.C., Paterson A.H. 2012. MCScanX: a toolkit for detection and evolutionary analysis of gene synteny and collinearity. *Nucleic Acids Res*. 40:e49–e49.
- Yang Y., Smith S.A. 2013. Optimizing de novo assembly of short-read RNA-seq data for phylogenomics. *BMC Genomics*. 14:328.
- Zhang C., Rabiee M., Sayyari E., Mirarab S. 2018. ASTRAL-III: polynomial time species tree reconstruction from partially resolved gene trees. *BMC Bioinformatics*. 19:523.

- Zhao T., Schranz M.E. 2019. Network-based microsynteny analysis identifies major differences and genomic outliers in mammalian and angiosperm genomes. *Proc. Natl. Acad. Sci.* 116:2165–2174.
- Zwick A., Regier J.C., Zwickl D.J. 2012. Resolving Discrepancy between Nucleotides and Amino Acids in Deep-Level Arthropod Phylogenomics: Differentiating Serine Codons in 21-Amino-Acid Models. *PLoS ONE*. 7:e47450.

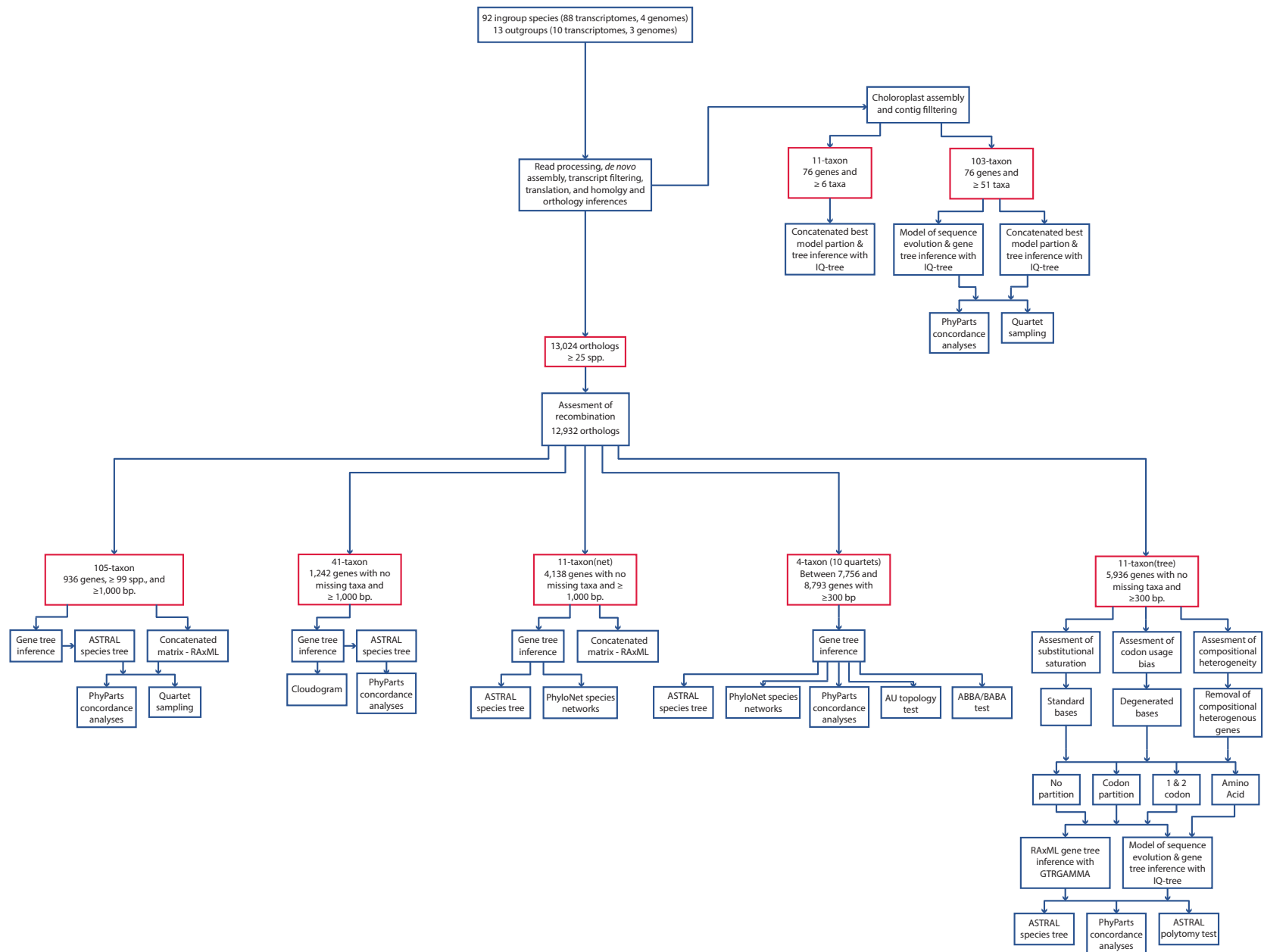


FIGURE S1. Overview of all datasets (red boxes) and analyses (blue boxes and arrows) in this study.

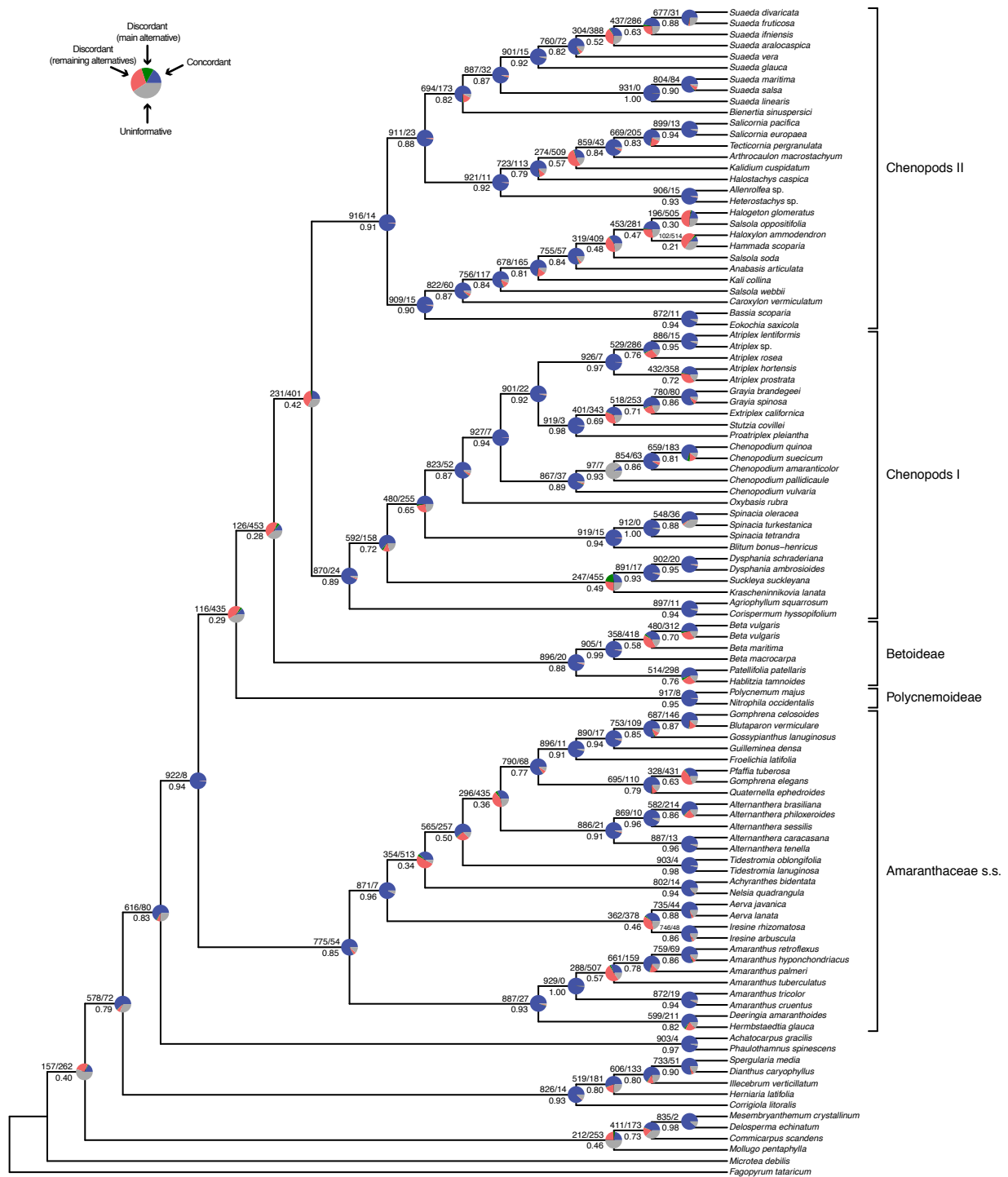


FIGURE S2. Maximum likelihood cladogram of Amaranthaceae s.l. inferred from RAxML analysis of the concatenated 936-nuclear gene supermatrix. Numbers above branches indicate the number of gene trees concordant/conflicting with that node in the species tree. Numbers below the branches are the Internode Certainty All (ICA) score. Pie charts on nodes present the proportion of gene trees that support that clade (blue), the proportion that support the main alternative bifurcation (green), the proportion that support the remaining alternatives (red), and the proportion (conflict or support) that have < 50% bootstrap support (gray).

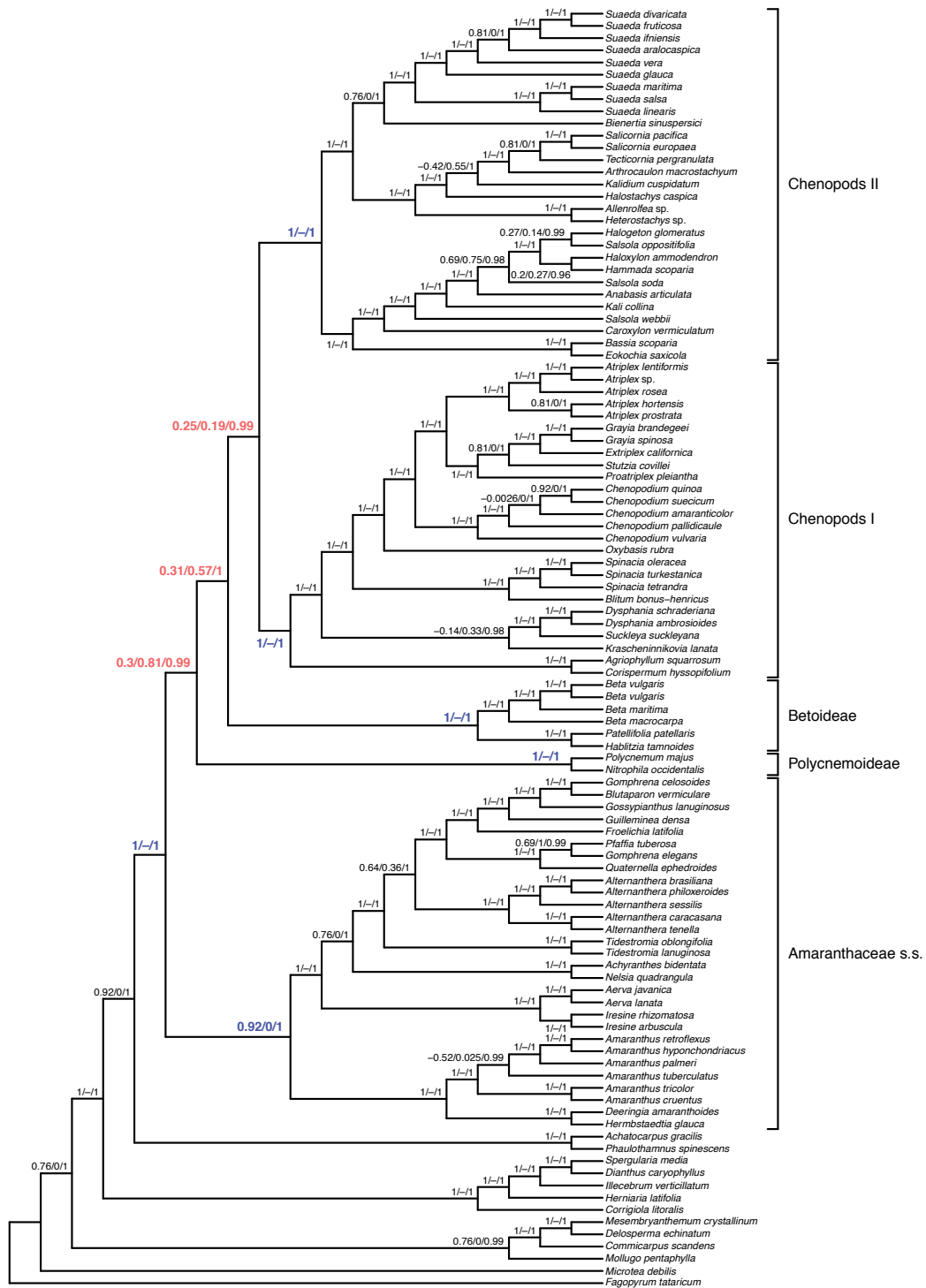


FIGURE S3. Maximum likelihood cladogram of Amaranthaceae s.l. inferred from RAxML analysis of the concatenated 936-nuclear gene supermatrix. Numbers above branches indicate the Quartet sampling internal node score. Quartet concordance/Quartet differential/ Quartet informativeness. Scores in blue indicate strong support for the species tree topology, while red scores indicate strong support for alternative topologies.

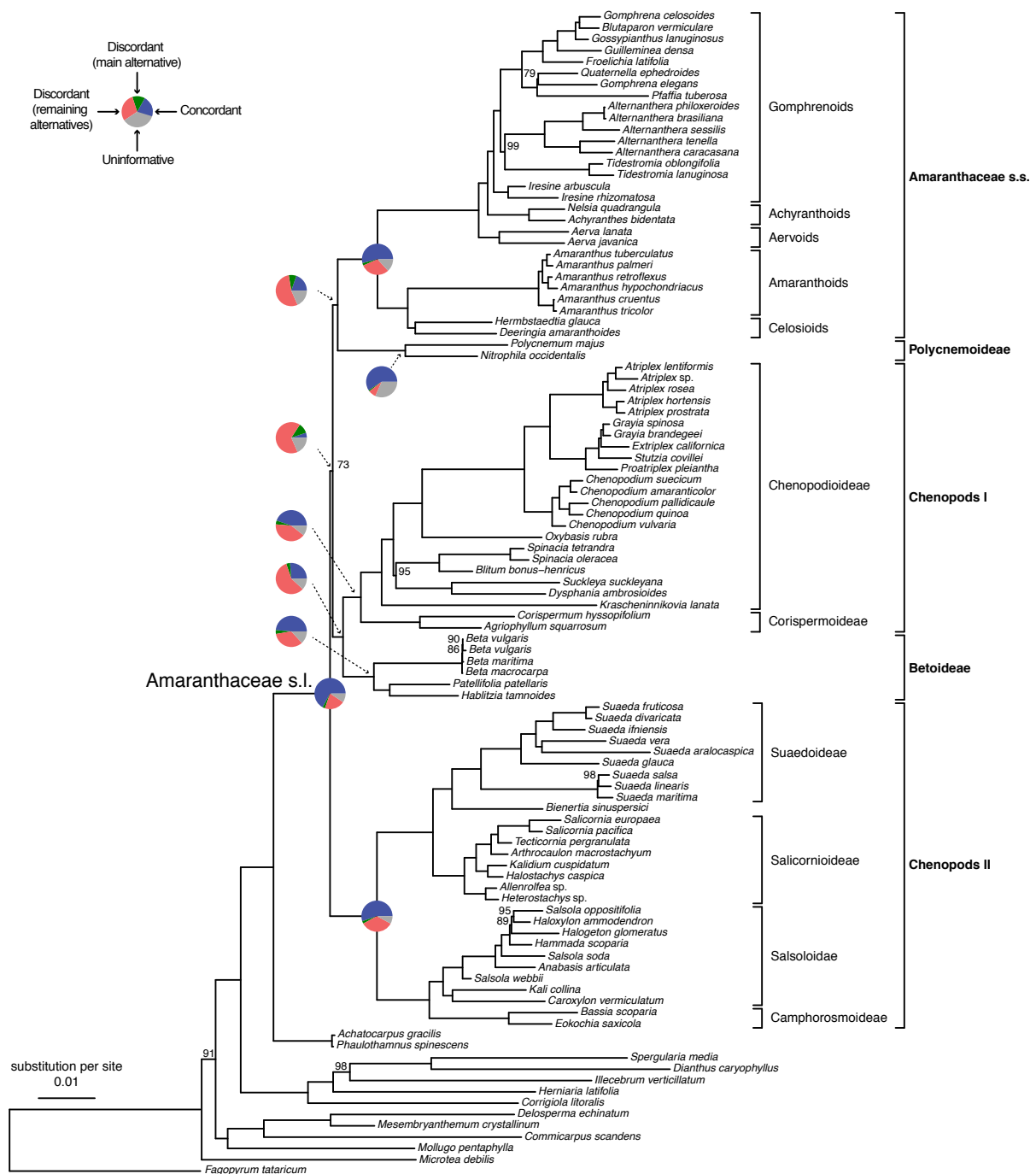


FIGURE S4. Maximum likelihood phylogeny of Amaranthaceae s.l. inferred from IQ-tree analysis of concatenated 76-plastid gene supermatrix. All nodes have full support (Bootstrap = 100) unless noted next to nodes. Pie charts present the proportion of gene trees that support that clade (blue), the proportion that support the main alternative bifurcation (green), the proportion that support the remaining alternatives (red), and the proportion (conflict or support) that have < 50% bootstrap support (gray). Only pie charts for major clades are shown (see Fig. S5 for all node pie charts). Branch lengths are in number of substitutions per site.

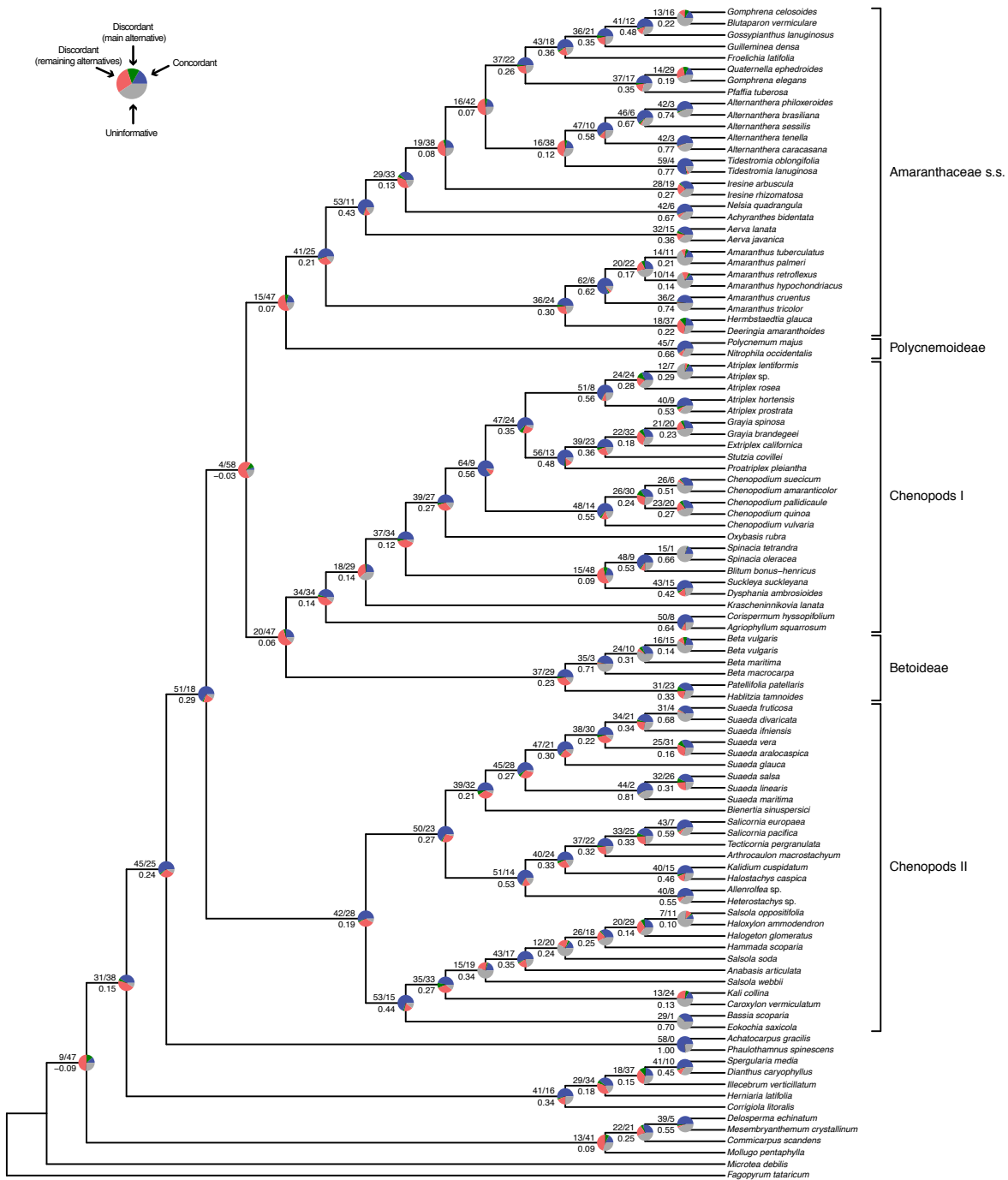


FIGURE S5. Maximum likelihood cladogram of Amaranthaceae s.l. inferred from IQ-tree analysis of concatenated 76-plastid gene supermatrix. Numbers above branches indicate the number of gene trees concordant/conflicting with that node in the species tree. Numbers below the branches are the Internode Certainty All (ICA) score. Pie charts on nodes present the proportion of gene trees that support that clade (blue), the proportion that support the main alternative bifurcation (green), the proportion that support the remaining alternatives (red), and the proportion (conflict or support) that have < 50% bootstrap support (gray).

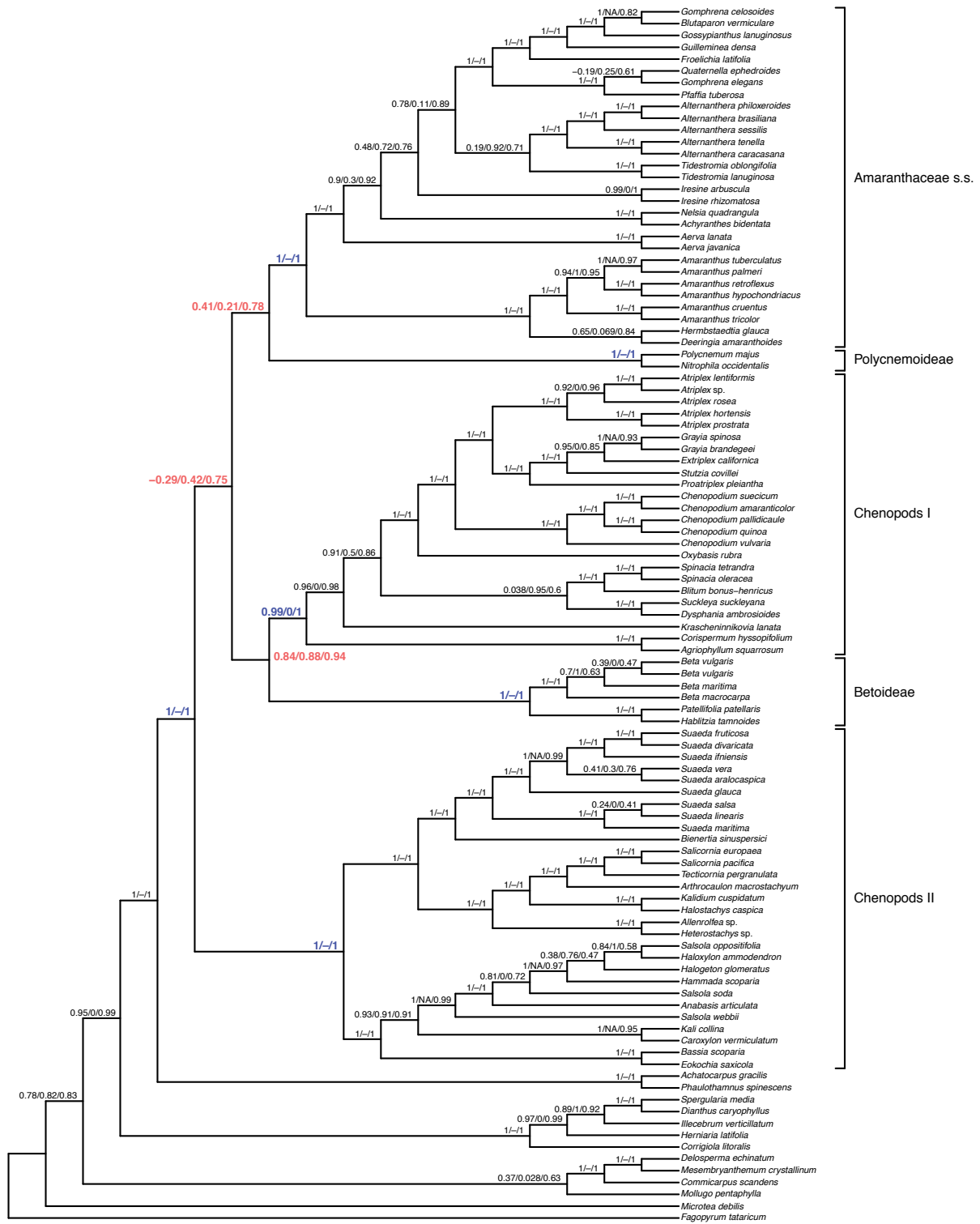


FIGURE S6. Maximum likelihood cladogram of Amaranthaceae s.l. inferred from IQ-tree analysis of concatenated 76-plastid gene supermatrix. Numbers above branches indicate the Quartet sampling internal node score. Quartet concordance/Quartet differential/ Quartet informativeness. Scores in blue indicate strong support for the species tree topology, while red scores indicate strong support for alternative topologies.

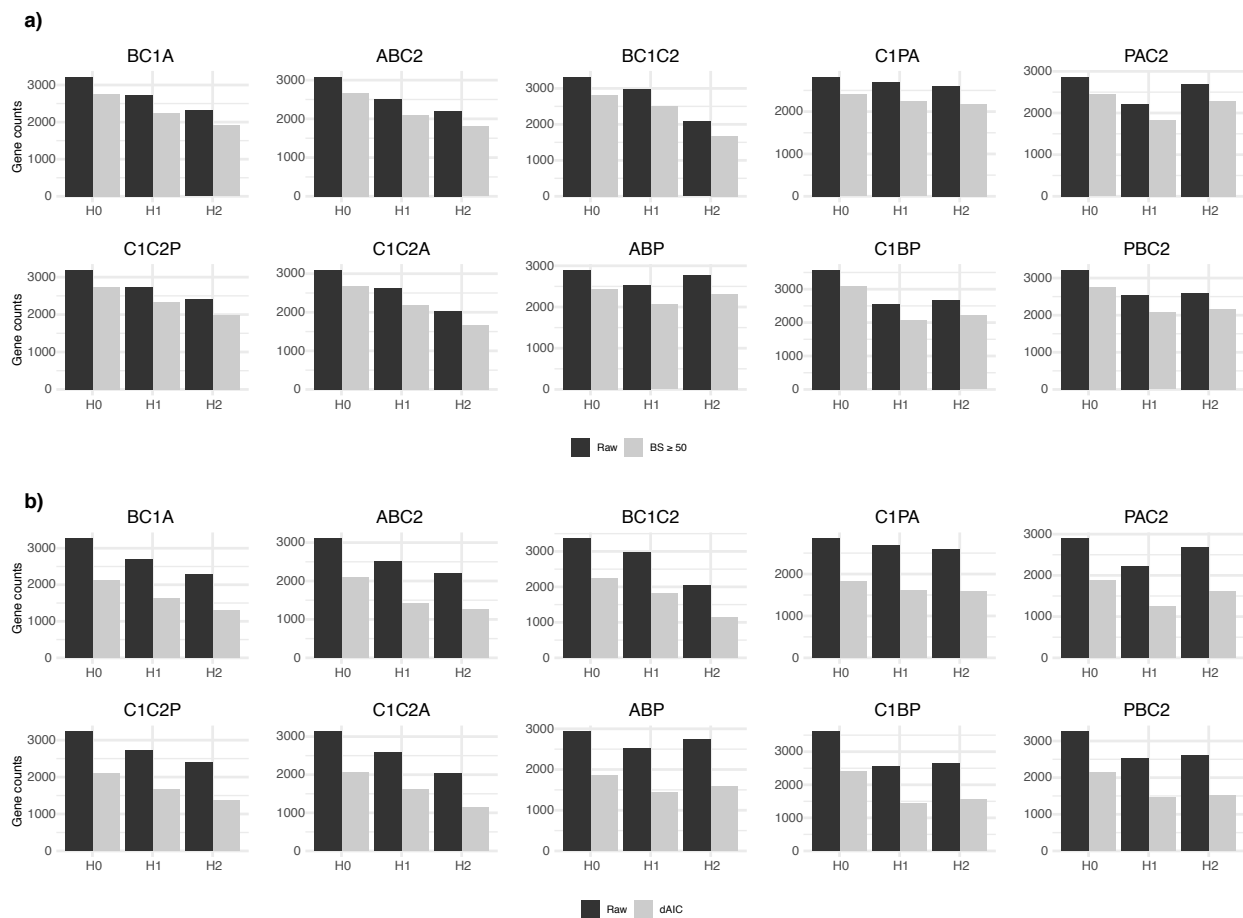


FIGURE S7. Counts of gene tree inferences for the 10 quartets from the five main clades of Amaranthaceae s.l. (a) Bars represent raw gene tree counts and counts of gene trees with bootstrap support ≥ 50 . Gene counts of constrained maximum likelihood searches for the 10 quartets from the five main clades of Amaranthaceae s.l. (b) Bars represent counts based on raw maximum likelihood scores and counts based on trees with significant support (trees with a delta corrected Akaike Information Criteria ($\Delta AICc$) ≥ 2 than the next best model). H0 represents the ASTRAL species tree of each quartet inferred. Each quartet is named following the species tree topology, where the first two species are sister to each other (all topologies can be found in Figure S6). A = Amaranthaceae. s.s. (*Amaranthus hypochondriacus*), B = Betoideae (*Beta vulgaris*), C1 = Chenopods I (*Chenopodium quinoa*), C2 = Chenopods II (*Caroxylum vermiculatum*), P = Polycnemoideae (*Polycnemonum majus*).

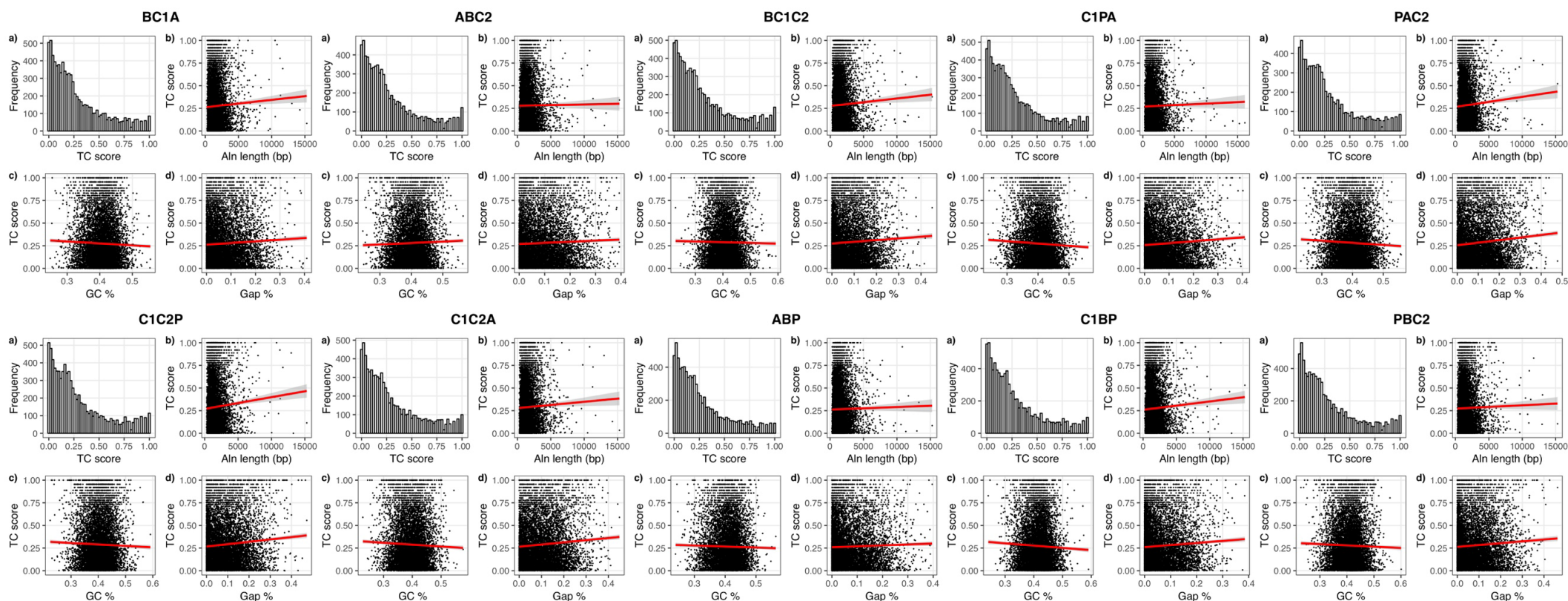


FIGURE S8. Alignment and tree scores for each of the 10 quartets from the five main clades of Amaranthaceae s.l. Quartet Tree Certainty (TC) score distribution (a) and its correlation with alignment length (b), alignment GC content (c), and alignment gap percentage (d). Quartets named following the ASTRAL species tree topology (see Figure 6 for quartet topologies). A = Amaranthaceae. s.s. (*Amaranthus hypochondriacus*), B = Betoideae (*Beta vulgaris*), C1 = Chenopods I (*Chenopodium quinoa*), C2 = Chenopods II (*Caroxylum vermiculatum*), P = Polycnemoideae (*Polycnemum majus*).



FIGURE S9. Best three species networks for the 10 quartets from the five main clades of Amaranthaceae s.l. Red and blue indicates the minor and major edges, respectively, of hybrid nodes. Number next to the branches indicates inheritance probabilities for each hybrid node. Network visualization with PhyloPlots (left) and network visualization with Dendroscope (right). Each quartet is named following the species tree topology, where the first two are sisters (all topologies can be found in Figure S6). A = Amaranthaceae. s.s. (*Amaranthus hypochondriacus*), B = Betoideae (*Beta vulgaris*), C1 = Chenopods I (*Chenopodium quinoa*), C2 = Chenopods II (*Caroxylum vermiculatum*), P = Polycnemoideae (*Polycnemum majus*).

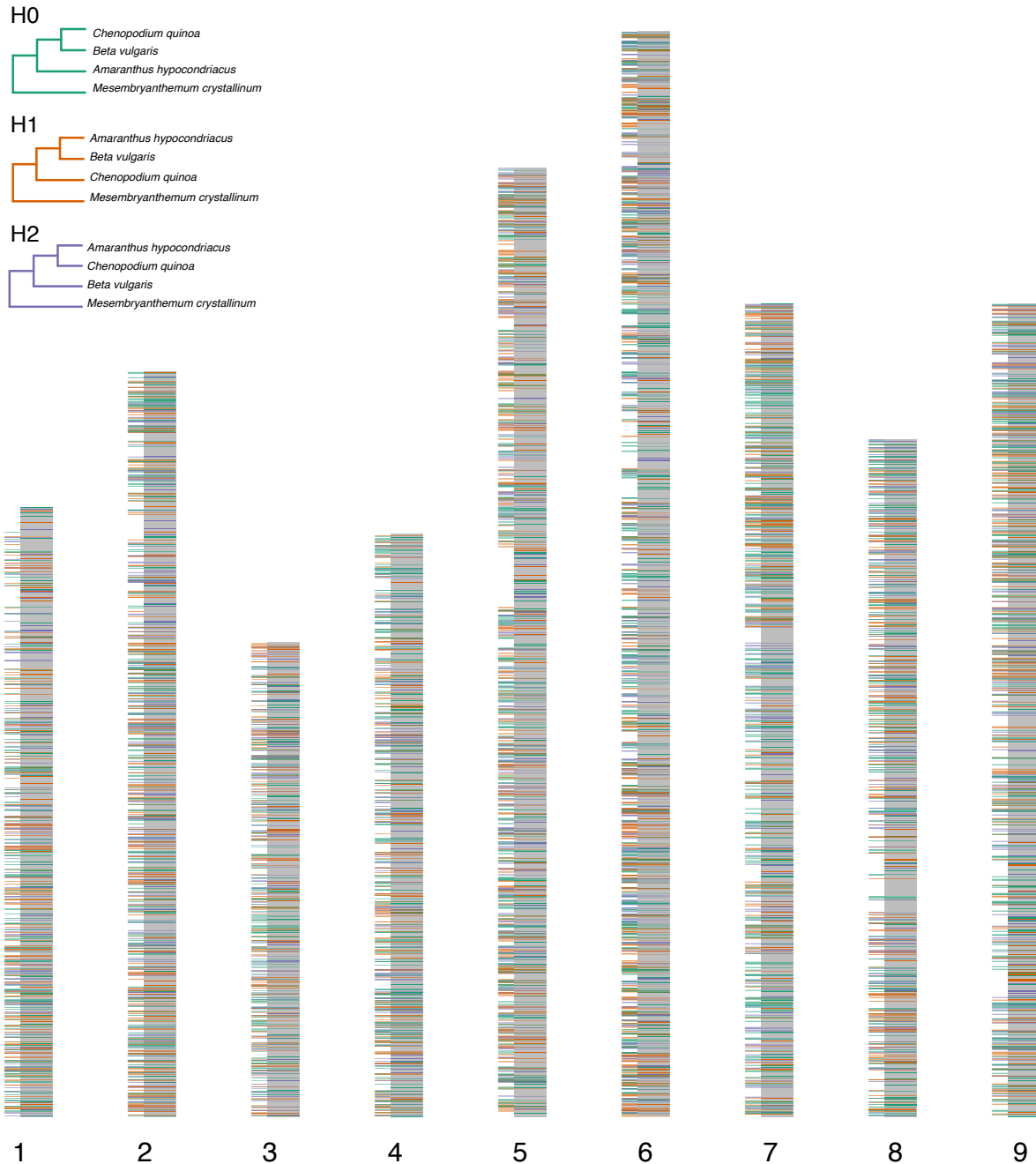
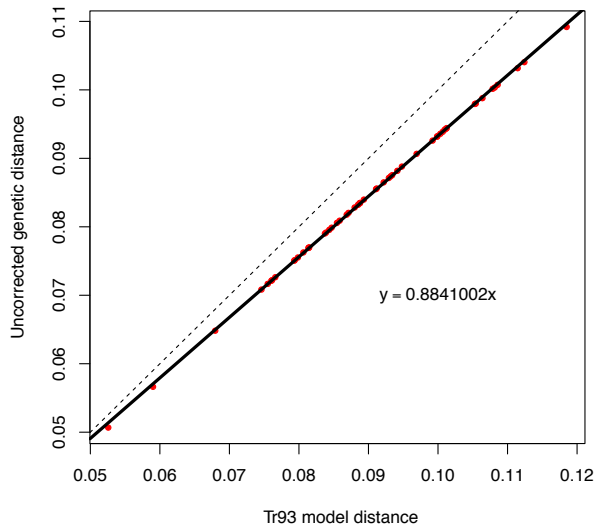


FIGURE S10. Chromosomes of *Beta vulgaris* with gene tree topologies from the quartet BC1A mapped. Each gene is colored according to gene tree topology (H0, H1, or H2). H0 represents the ASTRAL species tree of the quartet. Longer colored lines along the chromosomes represent syntenic genes (6,941) between *Beta vulgaris* and *Mesembryanthemum crystallinum*. Grey represents genes not present in the ortholog set of the quartet BC1A. A = Amaranthaceae. s.s. (*Amaranthus hypochondriacus*), B = Betoideae (*Beta vulgaris*), C1 = Chenopods I (*Chenopodium quinoa*), C2 = Chenopods II (*Caroxylum vermiculatum*), P = Polycnemoideae (*Polycnemonum majus*).

a) First and second codon positions



b) Only third codon position

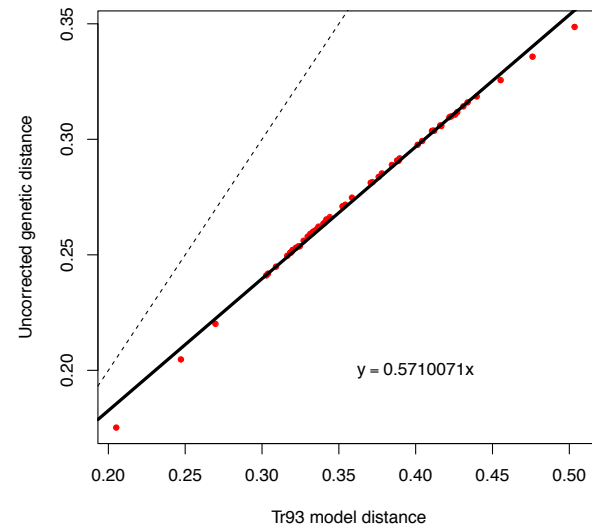
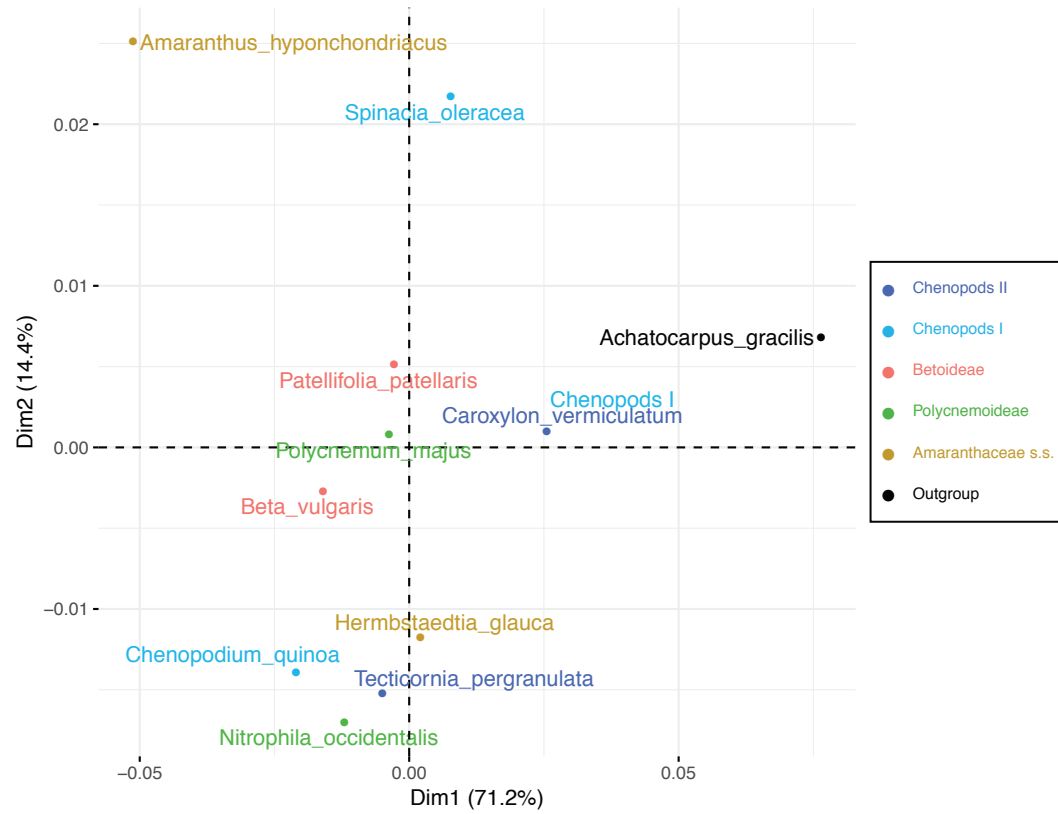


FIGURE S11. Saturation plots from the 11-taxon(tree) concatenated alignment. a) Saturation analysis for the first and second codon positions, and b) saturation analyses for the third codon position. Dotted lines represent expected unsaturated curves, and solid lines represent the observed saturation curves.

a) RSCU - Species



b) RSCU - Codons

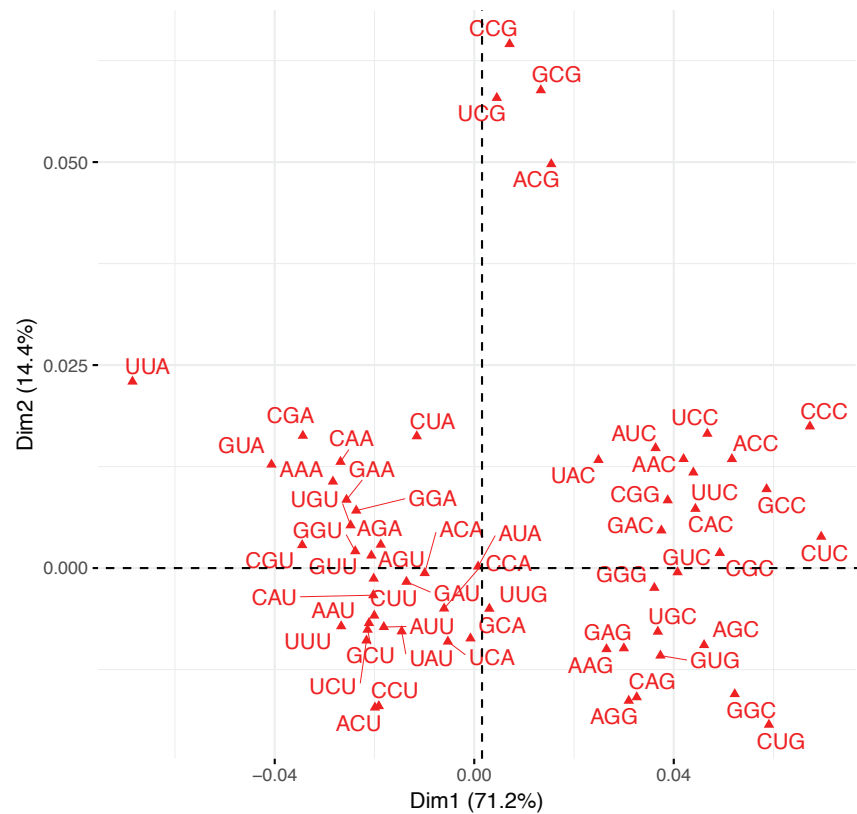


FIGURE S12. Correspondence analyses results of the Synonymous Codon Usage (RSCU) of the 11-taxon(tree) concatenated alignment. Results by a) species and (b) codons.

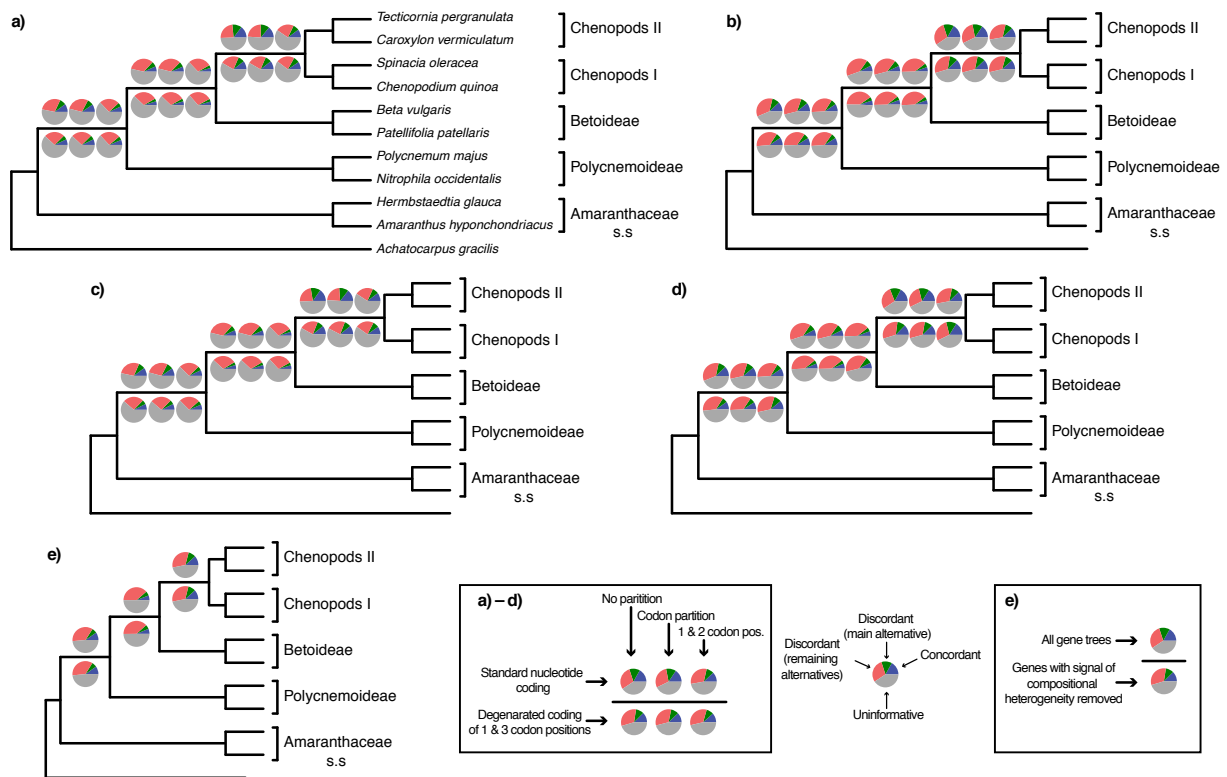


FIGURE S13. ASTRAL species trees from the 11-taxon(net) dataset estimated from gene trees inferred using multiple data schemes. a) Gene trees inferred with RAxML with a GTR-GAMMA model. b) Gene trees inferred with IQ-tree allowing for automatic model selection of sequence evolution. c) Gene trees inferred with RAxML with a GTR-GAMMA model and removal of genes that had signal of compositional heterogeneity. d) Gene trees inferred with IQ-tree allowing for automatic model selection of sequence evolution and removal of genes that had signal of compositional heterogeneity. a–d) Gene trees were inferred with no partition, codon partition (first and second codon, and third codon) and, only first and second codon positions (third codon position removed and no partition). Gene trees were inferred using codon alignments with standard nucleotide coding, and alignments with degenerated coding of the first and third codon positions. e) All gene trees and gene trees after removal of genes that had signal of compositional heterogeneity, inferred with IQ-tree using amino acid sequences allowing for automatic model selection of sequence evolution. Pie charts on nodes present the proportion of gene trees that support that clade (blue), the proportion that support the main alternative bifurcation (green), the proportion that support the remaining alternatives (red), and the proportion (conflict or support) that have < 50% bootstrap support (gray).

Table S2. Voucher information of newly sequenced transcriptions

Family	Subfamily	Species code	Genus	Species	Authority name	Voucher information	Locality	Growth condition	Tissue	RNA extraction	RNA-seq library preparation	Raw read pairs	Filtered nuclear read pairs	Filtered organelle read pairs
Amaranthaceae s.l.	Betulaceae	Habitag	<i>Aru</i>	<i>teigaria</i>	L.	Unvouchered	Cultivated at Botanical Garden University Mainz, orig. coll. Bulgaria. Living Collection	Cultivated at Botanical Garden University Mainz	Leaf	QIAGEN RNasy Plant Mini Kit with in-column DNase digestion by Delphine Terfalkis at Kadereit Lab Jun 2018	TruSeq Stranded Total RNA Library Prep-Plant with RiboZero by U. Minnesota Genomics Center Aug 2018	22,125,749	12,050,145	9,280,410
Amaranthaceae s.l.	Betulaceae	Habitag	<i>Wahlbergia</i>	<i>immundula</i>	(C.A. Mey.) Donag.	Kadereit, G. s.n. (MIG 027642)	Cultivated at Botanical Garden University Mainz, seeds obtained from a nursery	Cultivated at Botanical Garden University Mainz	Leaf	QIAGEN RNasy Plant Mini Kit with in-column DNase digestion by Delphine Terfalkis at Kadereit Lab Jun 2018	TruSeq Stranded Total RNA Library Prep-Plant with RiboZero by U. Minnesota Genomics Center Aug 2018	18,820,868	6,781,186	7,402,286
Amaranthaceae s.l.	Betulaceae	Pemp	<i>Pavlovigia</i>	<i>pauciflora</i>	(Moq.) A.J. Scott, Foster-Lloyd & J.T. Williams	H. Freitag 00031 (MIG 013502)	SW Morocco. Living Collection Botanic Garden Mainz 98	Cultivated at Botanical Garden University Mainz	Leaf	QIAGEN RNasy Plant Mini Kit with in-column DNase digestion by Delphine Terfalkis at Kadereit Lab Jun 2018	TruSeq Stranded Total RNA Library Prep-Plant with RiboZero by U. Minnesota Genomics Center Aug 2018	20,112,651	12,691,482	6,396,902
Amaranthaceae s.l.	Colocleth	Ducanar	<i>Ducanaria</i>	<i>amarocephala</i>	(L.) Moench	Milkenstein Seed Bank 301198 (MIG 023017)	Orig. coll. China, Yunnan. Living Collection Botanic Garden Mainz 344	Cultivated at Botanical Garden University Mainz	Leaf	QIAGEN RNasy Plant Mini Kit with in-column DNase digestion by Delphine Terfalkis at Kadereit Lab Jun 2018	TruSeq Stranded Total RNA Library Prep-Plant with RiboZero by U. Minnesota Genomics Center Aug 2018	21,713,222	17,238,976	3,069,492
Amaranthaceae s.l.	Colocleth	Hartig	<i>Hartigia</i>	<i>trichocarpa</i>	Glava	Milkenstein Seed Bank 140498 (MIG 023036)	Orig. coll. South Africa, Cape Province. Living Collection Botanic Garden Mainz 318	Cultivated at Botanical Garden University Mainz	Leaf	QIAGEN RNasy Plant Mini Kit with in-column DNase digestion by Delphine Terfalkis at Kadereit Lab Jun 2018	TruSeq Stranded Total RNA Library Prep-Plant with RiboZero by U. Minnesota Genomics Center Aug 2018	21,285,421	16,726,894	3,619,788
Amaranthaceae s.l.	Gomphosporaceae	Goenck	<i>Gomphospora</i>	<i>californica</i>	Mart.	Agoston, L. 41 (58)	Argentina, Misiones, Leandro N. Alem.	Cultivated at Botanical Garden University Mainz	Leaf	QIAGEN RNasy Plant Mini Kit with in-column DNase digestion by Delphine Terfalkis at Kadereit Lab Jun 2018	TruSeq Stranded Total RNA Library Prep-Plant with RiboZero by U. Minnesota Genomics Center Aug 2018	21,432,362	14,924,209	5,402,969
Amaranthaceae s.l.	Gomphosporaceae	Goenck	<i>Gomphospora</i>	<i>obliqua</i>	Mart.	E. Nieri (MIG 027640)	Argentina, Buenos Aires, Isidre, Cultivada en el vivero de Ribera norte.	Cultivated at Botanical Garden University Mainz	Leaf	QIAGEN RNasy Plant Mini Kit with in-column DNase digestion by Delphine Terfalkis at Kadereit Lab Jun 2018	TruSeq Stranded Total RNA Library Prep-Plant with RiboZero by U. Minnesota Genomics Center Aug 2018	21,301,222	14,457,205	5,711,422
Amaranthaceae s.l.	Gomphosporaceae	Pfand	<i>Pfandia</i>	<i>rubra</i>	Agoston, L. 51 (58)	Argentina, Corrientes, Santo Tomé.	Cultivated at Botanical Garden University Mainz	Leaf	QIAGEN RNasy Plant Mini Kit with in-column DNase digestion by Delphine Terfalkis at Kadereit Lab Jun 2018	TruSeq Stranded Total RNA Library Prep-Plant with RiboZero by U. Minnesota Genomics Center Aug 2018	21,238,253	11,557,156	8,516,484	
Amaranthaceae s.l.	Gomphosporaceae	Quashe	<i>Quasheia</i>	<i>epiphytica</i>	Podoc.	Milkenstein Seed Bank 107437 (MIG 023038)	Orig. coll. Brazil, Bahia Palmiras. Living Collection Botanic Garden Mainz 270	Cultivated at Botanical Garden University Mainz	Leaf	QIAGEN RNasy Plant Mini Kit with in-column DNase digestion by Delphine Terfalkis at Kadereit Lab Jun 2018	TruSeq Stranded Total RNA Library Prep-Plant with RiboZero by U. Minnesota Genomics Center Aug 2018	21,081,847	11,913,784	8,293,073
Amaranthaceae s.l.	Gomphosporaceae	Trop1813	<i>Tropaeolum</i>	<i>chilense</i>	(S. Wats.) Standl.	CUDG 2016029	Cultivated at Rancho Santa Ana Botanical Garden	Cultivated at Rancho Santa Ana Botanic Garden	Leaf?	Cambridge Sep 2016	KAPA Stranded RNA-Seq Library Preparation Kit (KK8420) with poly-A enrichment by Ning Wang at Smith Lab Oct 13, 2016	26,708,058	20,480,127	1,022,721
Chenopodiaceae	Chenopodiaceae	Chenoban	<i>Atriplex</i>	<i>hirsuta</i>	(L.) C.A. Mey.	Kadereit, G. s.n. (MIG 027643)	Cultivated at Botanical Garden University Mainz.	Cultivated at Botanical Garden University Mainz	Leaf	QIAGEN RNasy Plant Mini Kit with in-column DNase digestion by Delphine Terfalkis at Kadereit Lab Jun 2018	TruSeq Stranded Total RNA Library Prep-Plant with RiboZero by U. Minnesota Genomics Center Aug 2018	20,383,537	13,483,745	5,683,389
Chenopodiaceae	Chenopodiaceae	Chenoban	<i>Chenopodium</i>	<i>rubrum</i>	L.	Kadereit, G. s.n. (MIG 027638)	Cultivated at Botanical Garden University Mainz. Seeds obtained from Botanical Garden Innsbruck (Austria). Living Collection Botanic Garden Mainz 281	Cultivated at Botanical Garden University Mainz	Flower bud	QIAGEN RNasy Plant Mini Kit and QIAGEN RNase-Free DNase Set by Alfonso Timonada at Brockington lab	TruSeq Stranded Total RNA Library Prep-Plant with RiboZero by U. Minnesota Genomics Center Aug 2018	21,539,488	11,880,777	7,538,649
Chenopodiaceae	Chenopodiaceae	Dysamb	<i>Dysphania</i>	<i>ambrosioides</i>	(L.) Moench & Clement	Milkenstein Seed Bank 57718 (MIG 023990)	Cultivated at the Botanical Garden Mainz, orig. coll. unknown.	Cultivated at Botanical Garden University Mainz	Leaf	QIAGEN RNasy Plant Mini Kit with in-column DNase digestion by Delphine Terfalkis at Kadereit Lab Jun 2018	TruSeq Stranded Total RNA Library Prep-Plant with RiboZero by U. Minnesota Genomics Center Aug 2018	21,342,486	14,081,344	5,073,626
Chenopodiaceae	Salsolinaceae	Heteroc	<i>Heterocallis</i>	<i>obovata</i>	Spag.	Kadereit, G. s.n. (MIG 027635)	Argentina, source seed exchange. Living Collection Botanic Garden Mainz 34	Cultivated at Botanical Garden University Mainz	Leaf	QIAGEN RNasy Plant Mini Kit with in-column DNase digestion by Delphine Terfalkis at Kadereit Lab Jun 2018	TruSeq Stranded Total RNA Library Prep-Plant with RiboZero by U. Minnesota Genomics Center Aug 2018	19,448,518	11,682,378	7,053,278
Chenopodiaceae	Suaeditaceae	Suaedit	<i>Suaeda</i>	<i>obovata</i>	Moq.	Unvouchered	Cultivated at the Botanical Garden Mainz, orig. coll. Comodoro Rivadavia, Chubut, Argentina; source seed exchange. Living Collection Botanic Garden Mainz 35	Cultivated at Botanical Garden University Mainz	Leaf and apical meristem	QIAGEN RNasy Plant Mini Kit and QIAGEN RNase-Free DNase Set by Alfonso Timonada at Brockington lab	TruSeq Stranded Total RNA Library Prep-Plant with RiboZero by U. Minnesota Genomics Center Aug 2018	20,571,773	15,100,442	4,298,598
Chenopodiaceae	Suaeditaceae	Suaedit	<i>Suaeda</i>	<i>florosa</i>	Cahill ex. Maire	H. Freitag 00022 (MIG 013577)	Cultivated at the Botanical Garden Mainz, orig. coll. SW Morocco, Marfif ca. 25 km behind NE Sidi Bici. Living Collection Botanic Garden Mainz 205 (MIG 027635)	Cultivated at Botanical Garden University Mainz	Leaf and apical meristem	QIAGEN RNasy Plant Mini Kit and QIAGEN RNase-Free DNase Set by Alfonso Timonada at Brockington lab	TruSeq Stranded Total RNA Library Prep-Plant with RiboZero by U. Minnesota Genomics Center Aug 2018	21,255,893	13,880,141	8,274,304
Chenopodiaceae	Suaeditaceae	Suaedit	<i>Suaeda</i>	<i>serotina</i>	Forsk. ex J.F. Gmel	Kadereit, G. s.n. (MIG 027641)	Cultivated at Botanical Garden Mainz, seeds obtained from Botanical Garden Lisbon (Portugal). Living Collection Botanic Garden Mainz 187	Cultivated at Botanical Garden University Mainz	Leaf and apical meristem	QIAGEN RNasy Plant Mini Kit and QIAGEN RNase-Free DNase Set by Alfonso Timonada at Brockington lab	TruSeq Stranded Total RNA Library Prep-Plant with RiboZero by U. Minnesota Genomics Center Aug 2018	22,667,424	12,662,690	8,652,755

Table S3. Chloroplast references used for plastome assembly and tree inference.

Family	Genus	Species	Authority name	Notes	Source database	Source code	Source reference	Source title
Aizoaceae	<i>Mesembryanthemum</i>	<i>crystallinum</i>	L.	Used as reference and and tree inference - OUTGROUP	GenBank	NC_029049	---	Yim, Ha, and Cushman, 2016. Unpublished.
Amaranthaceae	<i>Amaranthus</i>	<i>hypochondriacus</i>	L.	Used as reference and and tree inference	GenBank	NC_030770	Chaney et al. 2016	The complete chloroplast genome sequences for four <i>Amaranthus</i> species (Amaranthaceae)
Betoideae	<i>Beta</i>	<i>vulgaris</i>	L.	Used as reference and and tree inference	GenBank	KR230391	Stadermann et al. 2015	SMRT sequencing only de novo assembly of the sugar beet (<i>Beta vulgaris</i>) chloroplast genome
Caryophyllaceae	<i>Dianthus</i>	<i>caryophyllus</i>	L.	Used as reference and and tree inference - OUTGROUP	GenBank	MG989277	Chen et al. 2018	Structural characteristic and phylogenetic analysis of the complete chloroplast genome of <i>Dianthus caryophyllus</i> .
Chenopodiaceae	<i>Bienertia</i>	<i>sinuspersici</i>	Akhani	Used as reference and and tree inference	GenBank	KU726550	Kim et al. 2016	The complete chloroplast genome sequence of <i>Bienertia sinuspersici</i>
Chenopodiaceae	<i>Chenopodium</i>	<i>quinoa</i>	Willd.	Used as reference and and tree inference	GenBank	NC_034949	Hong et al. 2017	Complete Chloroplast Genome Sequences and Comparative Analysis of <i>Chenopodium quinoa</i> and <i>C. album</i> .
Chenopodiaceae	<i>Haloxylon</i>	<i>persicum</i>	Bunge ex Boiss. & Buhse	Used only as assembly reference	GenBank	NC_027669	Dong et al. 2016	Comparative analysis of the complete chloroplast genome sequences in psammophytic <i>Haloxylon</i> species (Amaranthaceae)
Chenopodiaceae	<i>Salicornia</i>	<i>europaea</i>	L.	Used only as assembly reference	GenBank	NC_027225	---	Ho et al., 2015. Unpublished.
Chenopodiaceae	<i>Spinacia</i>	<i>oleracea</i>	L.	Used as reference and and tree inference	GenBank	NC_002202	Schmitz-Linneweber et al. 2001	The plastid chromosome of spinach (<i>Spinacia oleracea</i>): complete nucleotide sequence and gene organization
Chenopodiaceae	<i>Suaeda</i>	<i>malacosperma</i>	Hara	Used only as assembly reference	GenBank	MG813535	Park et al. 2018	The complete plastid genome of <i>Suaeda malacosperma</i> (Amaranthaceae/Chenopodiaceae), a vulnerable halophyte in coastal regions of Korea and Japan
Montiaceae	<i>Cistanthe</i>	<i>longiscapa</i>	(Barnéoud) Carolin ex Hershk.	Used only as assembly reference	GenBank	NC_035140	Stroll et al. 2017	Development of microsatellite markers and assembly of the plastid genome in <i>Cistanthe longiscapa</i> (Montiaceae) based on low-coverage whole genome sequencing
Polygonaceae	<i>Fagopyrum</i>	<i>tataricum</i>	(L.) Gaertn.	Used as reference and and tree inference - OUTGROUP	GenBank	NC_027161	Cho et al. 2015	Complete Chloroplast Genome Sequence of Tartary Buckwheat (<i>Fagopyrum tataricum</i>) and Comparative Analysis with Common Buckwheat (<i>F. esculentum</i>).

Table S4. Assembled plastid CDS and alignment stats.

Gene name	No. taxa	Alignment length	No. nucleotides	% missing data
<i>accD</i>	74	1452	99245	7.6%
<i>atpA</i>	100	1529	152424	0.3%
<i>atpB</i>	93	1500	136630	2.1%
<i>atpE</i>	81	408	32895	0.5%
<i>atpF</i>	100	555	54953	1.0%
<i>atpH</i>	100	246	24600	0.0%
<i>atpI</i>	100	744	73977	0.6%
<i>ccsA</i>	64	972	61080	1.8%
<i>cemA</i>	93	690	63866	0.5%
<i>clpP</i>	70	588	34555	16.0%
<i>infA</i>	95	234	22196	0.2%
<i>matK</i>	73	1588	102683	11.4%
<i>ndhA</i>	92	1099	95991	5.1%
<i>ndhB</i>	81	777	58130	7.6%
<i>ndhC</i>	98	363	35574	0.0%
<i>ndhD</i>	73	1505	103259	6.0%
<i>ndhE</i>	62	306	18777	1.0%
<i>ndhF</i>	51	2291	99017	15.3%
<i>ndhG</i>	63	531	33326	0.4%
<i>ndhH</i>	91	1182	106082	1.4%
<i>ndhI</i>	76	513	38416	1.5%
<i>ndhJ</i>	95	477	45315	0.0%
<i>ndhK</i>	100	684	67804	0.9%
<i>petA</i>	96	963	91872	0.6%
<i>petB</i>	64	642	41072	0.0%
<i>petD</i>	95	479	45372	0.3%
<i>petG</i>	76	114	8664	0.0%
<i>petL</i>	72	96	6896	0.2%
<i>petN</i>	53	90	4770	0.0%
<i>psaA</i>	101	2254	225017	1.2%
<i>psaB</i>	100	2205	218615	0.9%
<i>psaC</i>	59	246	14514	0.0%
<i>psaI</i>	93	111	10323	0.0%
<i>psaJ</i>	73	135	9844	0.1%
<i>psbA</i>	80	1066	85280	0.0%
<i>psbB</i>	100	1527	151853	0.6%
<i>psbC</i>	103	1435	146143	1.1%
<i>psbD</i>	101	1009	101607	0.3%
<i>psbE</i>	94	252	23688	0.0%
<i>psbF</i>	94	120	11280	0.0%
<i>psbH</i>	77	222	17045	0.3%
<i>psbI</i>	67	111	7417	0.3%
<i>psbJ</i>	94	123	11562	0.0%

Gene name	No. taxa	Alignment length	No. nucleotides	% missing data
<i>psbK</i>	67	180	12058	0.0%
<i>psbL</i>	94	117	10971	0.2%
<i>psbM</i>	56	105	5880	0.0%
<i>psbN</i>	76	132	10032	0.0%
<i>psbT</i>	98	108	10497	0.8%
<i>psbZ</i>	81	189	15309	0.0%
<i>rbcL</i>	96	1428	134885	1.6%
<i>rpl2</i>	85	825	70105	0.0%
<i>rpl14</i>	95	366	34769	0.0%
<i>rpl16</i>	92	358	32868	0.2%
<i>rpl20</i>	85	387	32821	0.2%
<i>rpl22</i>	88	599	50296	4.6%
<i>rpl23</i>	82	268	21845	0.6%
<i>rpl32^a</i>	23	174	3956	1.1%
<i>rpl33</i>	67	201	13402	0.5%
<i>rpl36</i>	99	114	11257	0.3%
<i>rpoA</i>	99	994	97641	0.8%
<i>rpoB</i>	71	3261	176067	24.0%
<i>rpoC1</i>	70	2049	129381	9.8%
<i>rpoC2</i>	74	4267	235989	25.3%
<i>rps2</i>	95	711	66704	1.2%
<i>rps3</i>	92	657	59822	1.0%
<i>rps4</i>	88	606	53206	0.2%
<i>rps7</i>	90	468	42069	0.1%
<i>rps8</i>	95	405	38475	0.0%
<i>rps11</i>	98	417	40855	0.0%
<i>rps12</i>	77	372	21630	24.5%
<i>rps14</i>	96	303	28948	0.5%
<i>rps15</i>	87	273	23680	0.3%
<i>rps16</i>	64	268	16793	2.1%
<i>rps18</i>	74	306	22618	0.1%
<i>rps19</i>	86	279	23640	1.5%
<i>ycf2^a</i>	46	6514	258235	13.8%
<i>ycf3</i>	93	515	43410	9.4%
<i>ycf4</i>	96	555	52771	1.0%

^aGene excluded from phylogenetic analyses due to low taxon occupancy

Table S5. Model selection between maximum number of reticulations in species networks searches.

Topology	Maximum number of reticulations allowed	Number of inferred reticulations	ln(L)	Parameters	Number of loci	AICc	ΔAICc	BIC	ΔBIC
Nuclear concatenated	NA	NA	-24486.331	19	4138	49048.847	20589.6635	49130.8939	20546.6229
ASTRAL	NA	NA	-23448.397	19	4138	46972.9794	18513.7959	47055.0262	18470.7552
cpDNA concatenated	NA	NA	-24568.333	19	4138	49212.8503	20753.6668	49294.8971	20710.6261
Network 1	1	1	-21177.791	21	4138	42439.8068	13980.6233	42530.4696	13946.1986
Network 2	2	2	-17275.625	23	4138	34643.5188	6184.33532	34742.7937	6158.52273
Network 3	3	2	-16741.991	23	4138	33576.2506	5117.06715	33675.5256	5091.25455
Network 4	4	3	-15415.8	25	4138	30931.9164	2472.73289	31039.7994	2455.52844
Network 5	5	5	-14171.38	29	4138	28459.1835	0	28584.271	0

Table S6. Model selection between quartet tree topologies and species networks. Trees correspond to each of the three possible quartet topologies where H0 is the ASTRAL quartet species tree. Networks correspond to the best three networks for searches with one hybridization event allowed.

Quartet ^a	Topology ^b	ln(L)	Parameters	Number of loci	AICc	Δ AICc	BIC	Δ BIC
BC1A	H0	-9014.809786	5	8258	18049.62684	24.73436754	18074.71426	14.70279692
	H1	-9072.456373	5	8258	18164.92002	140.0275408	18190.00743	129.9959702
	H2	-9073.888783	5	8258	18167.78484	142.8923611	18192.87225	132.8607905
	Net 1	-8998.43945	7	8258	18024.89248	0	18060.01146	0
	Net 2	-8998.439526	7	8258	18024.89263	0.000151947	18060.01162	0.000151947
	Net 3	-8998.441478	7	8258	18024.89653	0.004056302	18060.01552	0.004056302
ABC2	H0	-8516.854413	5	7811	17053.71651	12.87079823	17078.52527	2.950887757
	H1	-8581.563051	5	7811	17183.13379	142.2880731	17207.94254	132.3681626
	H2	-8582.670875	5	7811	17185.34944	144.5037223	17210.15819	134.5838118
	Net 1	-8506.415681	7	7811	17040.84572	0	17075.57438	0
	Net 2	-8506.415769	7	7811	17040.84589	0.000176519	17075.57456	0.000176519
	Net 3	-8506.42071	7	7811	17040.85577	0.010057548	17075.58444	0.010057548
BC1C2	H0	-9140.191425	5	8385	18300.39001	156.347016	18325.55385	146.2848258
	H1	-9201.981045	5	8385	18423.96925	279.9262567	18449.13309	269.8640665
	H2	-9214.405292	5	8385	18448.81775	304.7747517	18473.98158	294.7125615
	Net 1	-9058.014812	7	8385	18144.04299	0	18179.26902	0
	Net 2	-9058.019338	7	8385	18144.05205	0.009052497	18179.27807	0.009052497
	Net 3	-9058.024046	7	8385	18144.06146	0.018468011	18179.28749	0.018468011
C1PA	H0	-8932.927759	5	8134	17885.8629	0	17910.87456	0
	H1	-8936.145955	5	8134	17892.29929	6.436391285	17917.31095	6.436391285
	H2	-8936.481125	5	8134	17892.96963	7.106730999	17917.98129	7.106730999
	Net 1	-8932.077808	7	8134	17892.1694	6.306498884	17927.18227	16.30771403
	Net 2	-8932.078011	7	8134	17892.16981	6.306905172	17927.18268	16.30812032
	Net 3	-8932.078714	7	8134	17892.17121	6.308310587	17927.18408	16.30952573
PAC2	H0	-8530.661274	5	7784	17081.33026	40.10000797	17106.12168	30.18704595
	H1	-8552.9448	5	7784	17125.89731	84.66706025	17150.68873	74.75409823

	H2	-8548.291438	5	7784	17116.59059	75.36033576	17141.382	65.44737374
	Net 1	-8506.607925	7	7784	17041.23025	0	17075.93463	0
	Net 2	-8506.609795	7	7784	17041.23399	0.00373969	17075.93837	0.00373969
	Net 3	-8506.618966	7	7784	17041.25233	0.02208072	17075.95671	0.02208072
C1C2P	H0	-9119.250871	5	8341	18258.50894	12.50997925	18283.64643	2.458344441
	H1	-9163.685997	5	8341	18347.37919	101.38023	18372.51669	91.32859519
	H2	-9164.83263	5	8341	18349.67246	103.6734974	18374.80995	93.62186263
	Net 1	-9108.992761	7	8341	18245.99896	0	18281.18809	0
	Net 2	-9108.994383	7	8341	18246.00221	0.003244509	18281.19133	0.003244509
	Net 3	-9108.994843	7	8341	18246.00313	0.0041636	18281.19225	0.0041636
C1C2A	H0	-8447.623029	5	7756	16915.2538	63.6063012	16940.02717	53.70057058
	H1	-8520.509174	5	7756	17061.02609	209.378593	17085.79946	199.4728624
	H2	-8522.764578	5	7756	17065.5369	213.889401	17090.31027	203.9836704
	Net 1	-8411.816521	7	7756	16851.6475	0	16886.3266	0
	Net 2	-8411.819912	7	7756	16851.65428	0.006781956	16886.33338	0.006781956
	Net 3	-8411.820308	7	7756	16851.65507	0.007573446	16886.33417	0.007573446
ABP	H0	-9008.115816	5	8206	18036.23895	3.307596079	18061.29474	-6.711300872
	H1	-9015.941176	5	8206	18051.88967	18.95831519	18076.94546	8.939418238
	H2	-9014.738462	5	8206	18049.48424	16.55288764	18074.54003	6.533990688
	Net 1	-9002.458846	7	8206	18032.93135	0	18068.00604	0
	Net 2	-9002.460142	7	8206	18032.93395	0.002592568	18068.00863	0.002592568
	Net 3	-9002.464397	7	8206	18032.94246	0.011102577	18068.01714	0.011102577
C1BP	H0	-9557.910518	5	8793	19135.82787	0	19161.22959	0
	H1	-9661.475396	5	8793	19342.95762	207.1297559	19368.35935	207.1297559
	H2	-9661.009687	5	8793	19342.0262	206.1983365	19367.42793	206.1983365
	Net 1	-9556.24034	7	8793	19140.49343	4.665563813	19176.05266	14.82306554
	Net 2	-9556.243036	7	8793	19140.49882	4.670955519	19176.05805	14.82845724
	Net 3	-9556.246261	7	8793	19140.50527	4.677405326	19176.0645	14.83490705
PBC2	H0	-9158.309463	5	8379	18336.62609	0	18361.78635	0
	H1	-9206.127177	5	8379	18432.26152	95.63542753	18457.42177	95.63542753
	H2	-9205.933131	5	8379	18431.87343	95.24733612	18457.03368	95.24733612

Net 1	-9158.016519	7	8379	18344.04642	7.42032489	18379.26742	17.48107897
Net 2	-9158.017286	7	8379	18344.04795	7.421858749	18379.26896	17.48261282
Net 3	-9158.017377	7	8379	18344.04813	7.422042036	18379.26914	17.48279611

^aEach quartet is named following the species tree topology, where the first two are sister. A = Amaranthaceae. s.s. (*Amaranthus hypochondriacus*), B = Betoideae (*Beta vulgaris*), C1 = Chenopods I (*Chenopodium quinoa*), C2 = Chenopods II (*Caroxylum vermiculatum*), P = Polycnemoideae (*Polycnemonum majus*).

^bAll quartet tree topologies can be found in Figure 5 and quartet network topologies in Figure S9.

Table S7. Gene count based on raw likelihood, Δ AIC, and AU topology test. Trees correspond to each of the tree possible quartet topologies^a where

Quartet ^b	Number of loci	Raw bipartitions		Bipartition with bootstrap ≥ 50				Raw likelihood			Δ AIC		AU topology test p-value			Equivocal	
		H0	H1	H2	H1	H2	H0	H0	H1	H2	H0	H1	H2				
BC1A	8258	3218	2723	2317	2753	2243	1912	3268	2692	2298	2130	1636	1295	130	98	47	7017
ABC2	7811	3083	2521	2207	2666	2100	1804	3108	2502	2201	2085	1415	1252	204	68	47	6605
BC1C2	8385	3319	2988	2078	2819	2516	1682	3365	2969	2051	2228	1817	1133	204	127	49	6945
C1PA	8134	2819	2705	2610	2407	2241	2173	2850	2684	2600	1822	1619	1592	95	80	98	6925
PAC2	7784	2866	2216	2702	2444	1837	2286	2896	2210	2678	1876	1255	1605	120	67	96	6603
C1C2P	8341	3190	2738	2413	2741	2346	1982	3232	2720	2389	2091	1655	1378	173	97	88	6935
C1C2A	7756	3095	2619	2042	2679	2193	1670	3132	2588	2036	2054	1624	1136	153	107	53	6466
ABP	8206	2897	2532	2777	2444	2061	2320	2932	2526	2748	1859	1434	1583	134	56	52	6697
C1BP	8793	3573	2544	2676	3085	2070	2212	3609	2542	2642	2397	1433	1555	162	55	71	7429
PBC2	8379	3216	2554	2609	2764	2073	2160	3257	2527	2595	2136	1454	1523	165	68	90	7062

^aAll topologies can be found in Figure 5.

^bEach quartet is named following the species tree topology, where the first two are sister. A = Amaranthaceae. s.s. (*Amaranthus hypochondriacus*), B = Betoideae (*Beta vulgaris*), C1 = Chenopods I (*Chenopodium quinoa*), C2 = Chenopods II (*Caroxylum vermiculatum*), P = Polycnemoideae (*Polycnemon majus*).

Table S8. Linear model results for correlation between quartet Tree consistency (TC) scores and alignment

Quartet ^a	Sample size	Alignment length		Gap content		GC content	
		R2	p-value	R2	p-value	R2	p-value
BC1A	8258	0.001147	0.002079	0.002228	1.78E-05	0.001008	0.003914
ABC2	7811	3.76E-05	0.5882	0.001275	0.001599	0.0006525	0.02397
BC1C2	8385	0.001113	0.002251	0.002348	9.02E-06	1.46E-04	0.2695
C1PA	8134	1.95E-04	0.2083	0.003885	1.85E-08	0.001725	0.0001788
PAC2	7784	2.06E-03	6.26E-05	0.008132	1.57E-15	0.001579	0.0004539
C1C2P	8341	0.002681	2.23E-06	0.005697	5.12E-12	0.0006883	0.01657
C1C2A	7756	0.0007874	1.35E-02	0.005023	4.14E-10	0.001103	0.003436
ABP	8206	0.0001394	0.2849	0.0008305	0.009037	0.0003169	0.1068
C1BP	8793	0.001477	0.0003123	0.003134	1.50E-07	0.001401	0.0004478
PBC2	8379	0.000225	0.1698	0.003343	1.18E-07	0.0005339	0.03442

^aEach quartet is named following the species tree topology, where the first two are sister. A = Amaranthaceae. s.s. (*Amaranthus hypochondriacus*), B = Betoideae (*Beta vulgaris*), C1 = Chenopods I (*Chenopodium quinoa*), C2 = Chenopods II (*Caroxylum vermiculatum*), P = Polycnemoideae (*Polycnemum majus*).

Table S9. ABBA/BABA test results of Amaranthaceae s.l. five main groups quartets.

Quartet (H0)^a	Number of loci	Sites in alignment	ABBA	BABA	Raw D-statistic	Z-score	P-value	Introgression direction
BC1A ^b	8258	12778649	287226	254617	0.06018164	41.1085	≤ 0.001	A↔C1
ABC2	7811	12105324	252772	376755	-0.1969463	124.4161	≤ 0.001	A↔C2
BC1C2	8385	13192317	306570	258349	0.08535914	54.59751	≤ 0.001	C1↔C2
C1PA ^b	8134	12635201	342350	286813	0.08827124	64.62297	≤ 0.001	A↔P
PAC2	7784	12049734	344726	405627	-0.08116313	42.88069	≤ 0.001	C2↔P
C1C2P ^b	8341	13127397	445384	276652	0.2336892	136.0151	≤ 0.001	C2↔P
C1C2A ^b	7756	12114778	396219	292561	0.1504951	101.3243	≤ 0.001	A↔C2
ABP	8206	12622625	276319	312060	-0.06074486	36.64264	≤ 0.001	A↔P
C1BP ^b	8793	13712853	273286	261620	0.02180944	18.08364	≤ 0.001	B↔P
PBC2	8379	13074019	217549	415616	-0.3128205	196.8972	≤ 0.001	C2↔P

^aEach quartet is named following the species tree topology, where the first two are sister. A = Amaranthaceae. s.s. (*Amaranthus hypochondriacus*), B = Betoideae (*Beta vulgaris*), C1 = Chenopods I (*Chenopodium quinoa*), C2 = Chenopods II (*Caroxylum vermiculatum*), P = Polycnemoideae (*Polycnemonum majus*). H0 topologies can be found in Figure 6

^bQuartet compatible with the complete 105-taxon species trees

Table S10. Anomaly zone limit calculations in 11-taxon species trees. Bold rows show pair of internodes in the anomaly zone when $y < a(x)$.

Species tree^a	Clade (x)^b	Clade (y)^b	x	y	a(x)
	(C1, C2)	(C1)	0.1467	2.722	0.1799
	(C1, C2)	(C2)	0.1467	2.1102	0.1799
No partition	((C1, C2), B)	(C1, C2)	0.1045	0.1467	0.3084
	((C1, C2), B)	(B)	0.1045	2.6081	0.3084
	(((C1, C2), B), P)	((C1, C2), B)	0.0846	0.1045	0.4003
	(((C1, C2), B), P)	(P)	0.0846	3.5424	0.4003

^aSpecies tree topology can be found in Figure 6.

^b B = Betoideae (*Beta vulgaris*), C1 = Chenopods I (*Chenopodium quinoa*), C2 = Chenopods II (*Caroxylum vermiculatum*), P = Polycnemoideae (*Polycnemonum majus*).